Composites: Part A 195 (2025) 108951

Contents lists available at ScienceDirect

Composites Part A

journal homepage: www.elsevier.com/locate/compositesa

An experimental investigation into the lightning strike response of Z-pinned composite laminates

Mudan Chen [a,*], Yu Zhou [b,*], Bing Zhang [a], Giuliano Allegri [a], Tomohiro Yokozeki [b], Stephen R. Hallett [a]

[a] Bristol Composites Institute, University of Bristol, Queen's Building, Bristol BS8 1TR, UK
[b] Department of Aeronautics and Astronautics, The University of Tokyo, 7-3-1 Hongo, Bunkyo-Ku, Tokyo 113-8656, Japan

GRAPHICAL ABSTRACT

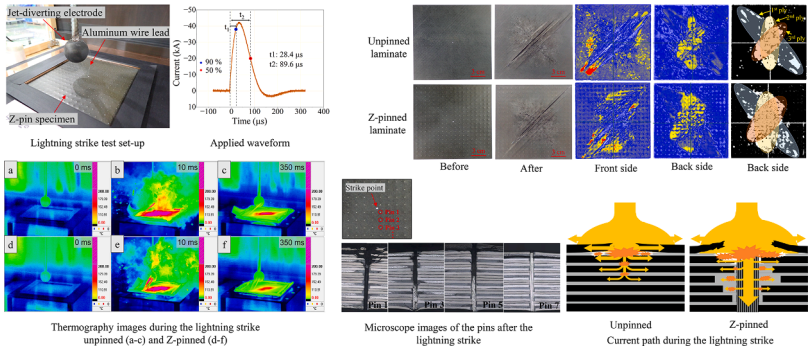

ARTICLE INFO

Keywords:
Multifunctional composites
Lightning strike
Z-pin
Laminate

ABSTRACT

Despite their outstanding mechanical performance and lightweight characteristics, carbon fibre reinforced polymer (CFRP) composites also have some limitations, notably: poor delamination resistance and vulnerability to lightning strikes. Z-pinning through-thickness reinforcement (TTR) technology addresses the first of these and this research represents the first investigation on the lightning strike damage response of Z-pinned CFRP composites. Two types of specimens were tested: unpinned and 0.1% carbon-fibre Z-pinned. Experimental results reveal that while Z-pinning enhances through-thickness electrical conductivity, it introduces new complexities. During lightning events, the intense current surge causes the carbon-fibre pins and adjacent resin pockets to decompose, resulting in localised damage, larger delamination areas, and reduced residual strength compared to unpinned laminates. Carbon-fibre Z-pinned laminates, however, dissipate heat more rapidly due to the efficient heat transfer facilitated by the pins. This study offers a novel perspective on the potential advantages and challenges associated with the application of Z-pinning in aircraft structures.

* Corresponding authors.
E-mail addresses: mudan.chen@bristol.ac.uk (M. Chen), yu-zhou1103@aastr.t.u-tokyo.ac.jp (Y. Zhou).

https://doi.org/10.1016/j.compositesa.2025.108951
Received 14 October 2024; Received in revised form 5 April 2025; Accepted 13 April 2025
Available online 14 April 2025

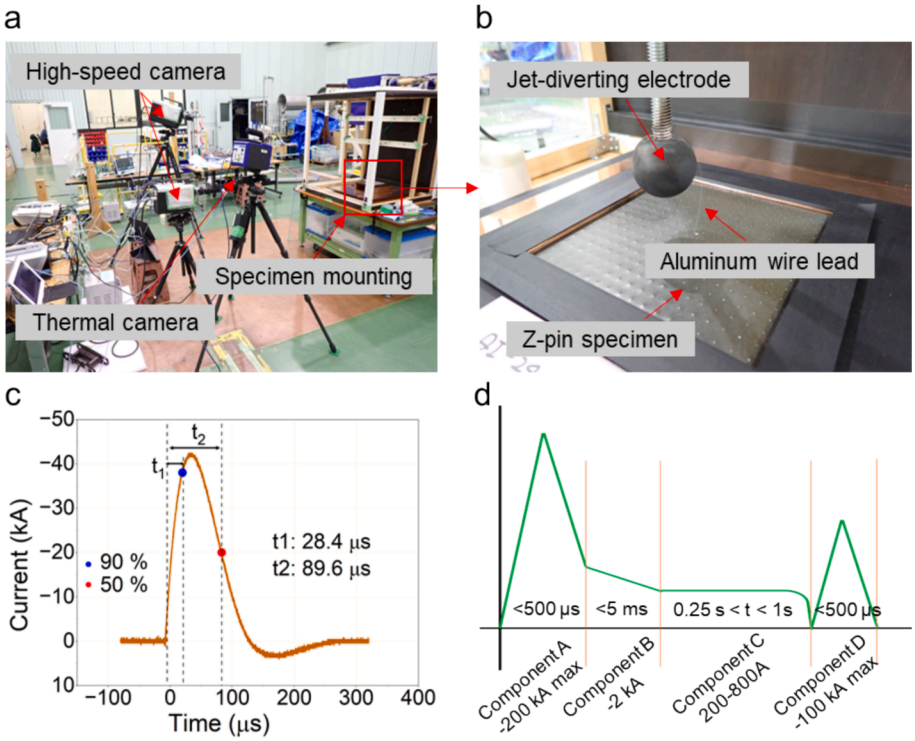

Fig. 1. (a) Experiment set-up configuration, (b) specimen mounting, (c) waveform applied in this study, and (d) lightning waveform defined by SAE ARP-5412B.

1. Introduction

Given their exceptional characteristics of high strength, stiffness, and low density, carbon fibre reinforced polymer (CFRP) composites are extensively utilised in the construction of lightweight structures. Nonetheless, it is important to address that CFRP composites do exhibit some inherent weaknesses.

Laminated fibre reinforced polymer composites can display poor delamination resistance. Through-thickness reinforcement (TTR) technologies, such as stitching [1], tufting [2], 3D weaving [3], and Z-pinning [4,5], can improve delamination resistance compared to unreinforced laminates. Z-pinning, in particular, is one of the only techniques that can be employed for prepreg materials, which involves the insertion of small-diameter rods or tubes through the thickness of the uncured composite [4,5]. Extensive research has demonstrated the effectiveness of Z-pinning in enhancing the interlaminar fracture toughness of composites under mode I, mode II, and mixed-mode loading conditions [6–11].

In contrast to carbon-fibre composites' advantages over metals in terms of their mechanical performance, carbon fibre has an electrical conductivity of approximately 6×10^4 S/m, which is about three orders of magnitude lower than that of metals. The epoxy resin matrix commonly used in aerospace applications further exhibits an even lower conductivity of 4.9×10^{-16} S/m [12–15]. Consequently, CFRP structures display high electrical resistance, with high anisotropy.

Within an airframe, a range of functions demand specific levels of electrical conductivity. This includes ensuring safety in the event of a short circuit occurring through structural components [15–17], as well as providing damage resistance against lightning strikes. In the realm of civil aviation, an airplane typically encounters lightning strikes approximately once or twice a year [13]. Lightning strikes can result in significant damage to unprotected CFRP structures. The substantial current generates heat within the laminate, elevating temperatures to points where the matrix resin decomposes or vaporizes. This damage is particularly pronounced in laminates with insufficient conductivity in the through-thickness direction [18,19]. The industry's approach involves integrating metallic materials into composite structures, such as meshes, foils, or interwoven fabrics attached to the surface of the component [12]. These protective elements effectively distribute current across the component's surface, thereby reducing or even preventing damage caused by lightning strikes.

In the literature, various alternative approaches have been explored to protect composites against lightning strikes, such as metal tufting [13,20], conductive resin [21,22], conductive coatings [23,24], and interleaves [25,26]. Incorporating stainless steel and copper tufting led to a remarkable increase in through-thickness electrical conductivity and resulted in a reduction of internal damage by approximately 75% and 90%, respectively, compared to laminates without reinforcement [20]. Similarly, silver-coated knitting yarns within non-crimp carbon fabrics (NCF) also achieved a 90% decrease in damage observed after a lightning strike test at a depth of 1 mm [13].

A growing interest has been shown in exploring the multi-functionality of Z-pins in recent years. Research has been conducted on monitoring delamination and enhancing the magnetic properties, as well as the electrical and thermal conductivities, of Z-pinned laminates [15,27–37]. In Ref. [29], it was found that Z-pins could enhance through-thickness electrical conductivity by up to six orders of magnitude. However, the pins did not improve the in-plane conductivity of composite laminates due to interfacial cracks around the pins. Recently, Ref. [15] demonstrated that Z-pins could reduce electrical resistance by two orders of magnitude for through-thickness fault currents and by up to one order of magnitude for in-plane fault currents. This enhanced electrical conductivity is attributed to the fibre crimping around the pin, independent of the pin material. The pins also effectively reduced the temperature rise caused by Joule heating.

Lightning strikes involve high-current impulses that occur within an extremely brief timeframe, which differs from the case of small constant currents in Ref. [15]. The current study investigated the response of Z-pinned CFRP laminate under lightning strikes for the first time and explores the underlying damage mechanisms. The most widely used carbon-fibre Z-pin material was selected here, to increase the through-thickness conductivity without significantly increasing weight. The

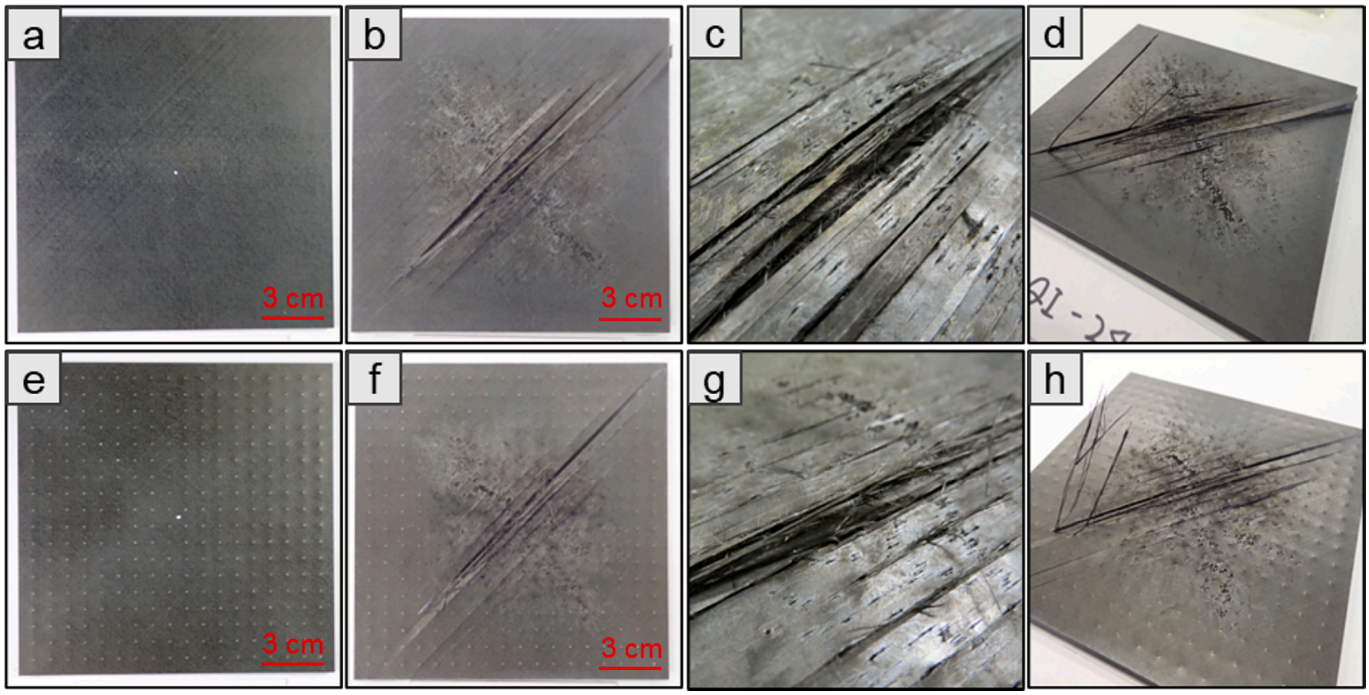

Fig. 2. Images of: unpinned (a-d) and Z-pinned (e-h) laminates, before (a, e) and after the simulated lightning strike.

specimen preparation and test set-up are introduced in Sections 2 and 3. The experimental results and damage mechanisms are discussed in Sections 4 and 5. Residual mechanical properties are given in Section 6. Conclusions and future work are summarised in Section 7.

2. Specimen preparation

The specimens employed in this study were made of UD M21/IMA prepreg (HexPly® M21/34%/UD194/IMA-12K) [38] following the QI stacking sequence of $[+45°/90°/-45°/0°]_{3S}$. The M21/IMA laminates are toughened with thermoplastic particles that lie in the resin rich layer between plies, serving as a separate interleaf [39]. Interleaving is a well-established method to enhance the interlaminar toughness of cured laminates [40], but a thick, non-conductive interleaf layer adversely affects electrical conductivity. T300/bismaleimide (BMI) pins with a diameter of 0.28 mm were employed to make Z-pinned specimens. The pin-to-pin distances were designed to be 8 mm, which gives a pinning areal density of 0.1%. Additionally, an unpinned control laminate was fabricated for comparison. Two types of specimens were prepared in total: 0.1% carbon-fibre Z-pinned and unpinned. One specimen of each type was tested for lightning strikes, and three specimens of each type were tested for electrical conductivity measurements.

The specimen manufacturing process primarily involves the following steps:

- Sequentially lay up the prepreg on an aluminum plate and debulk for 15 min in a vacuum bag after every four plies.
- Soften the laminate using a hot plate beneath it and manually insert pins through the laminate's thickness (for Z-pinned specimens).
- Cure the laminate in an autoclave following a modified Hexcel cure cycle [38], which includes extending the dwelling stage by 30 min to account for the presence of silicon rubbers placed on the top and bottom of the laminate for pin-end protection [15,41].
- Cut individual samples from the cured laminate using a diamond saw.

After cure, each ply has a nominal thickness of 0.188 mm, resulting in a total specimen thickness of 4.5 mm. The specimens for lightning strike tests have dimensions of 150 × 150 × 4.5 mm^3 (length × width × thickness), while those for electrical conductivity measurements are 16 × 16 × 4.5 mm^3, with each containing four pins.

3. Lightning strike test set-up

The simulated lightning strike test was carried out via a high-impulse current generator (Otowa Electric Co.) owned by SHODEN Co, Ltd. (Sitama, Japan). Fig. 1(a, b) shows the experiment configuration and specimen set-up before the strike. The specimen was clamped with a grounded copper frame-type jig, thereby completing the impulse generator's circuit. A jet-diverting electrode recommended by SAE ARP 5416A was used in the test to simulate a natural lightning event [42]. An aluminium wire lead was connected to the electrode to lead the electrical current to the test subject, and the distance between the tip of the wire and the test subject was 2 mm. A high-speed camera (Hyper vision HPV-X2, Shimadzu), and a thermography camera (SC 7600, FLIR, Inc.) were used to observe the simulated lightning discharge process. An electrical current of −40 kA (Fig. 1(c)) is applied during the strike test, delivering an action integral of 9.6 × 10^4 A^2 s. This corresponds to a modified component A waveform, as defined by SAE ARP-5421B (Fig. 1 (d)), representing the first return stroke in a lightning event.

4. Experimental results

4.1. Visual damage

Fig. 2 compares the visual damage of the control and Z-pinned laminates before and after the simulated lightning strike. Two panels exhibit a similar behaviour, characterised by fibre peeling along the fibre direction, multiple-layer damage at the centre of the stroke, and thermal ablations resulting from the current traveling along the surface. These are typical lightning strike damage behaviours that have been observed in many other works [18,43,44].

The electrical current was primarily conducted along the fibres, while also went into the panel by the dielectric breakdown of resin matrix between layers. The Joule heating effect caused severe decomposition of the epoxy resin matrix due to its poor electrical conductivity.

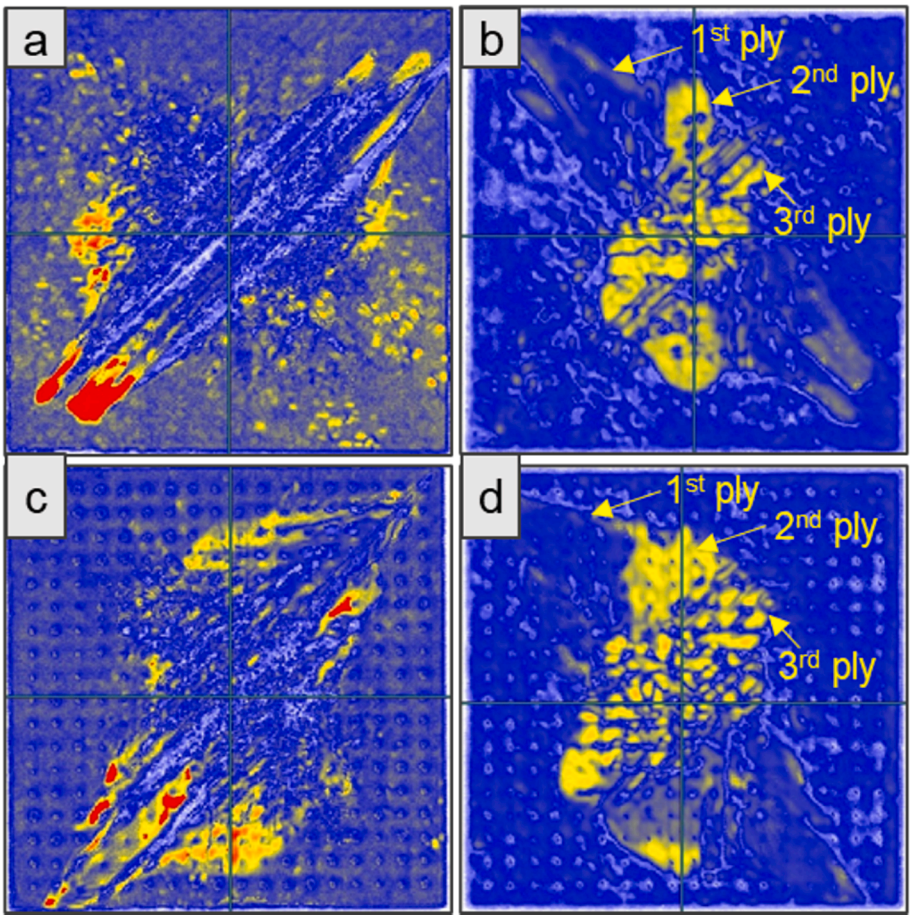

Fig. 3. Ultrasonic NDI images: (a, c) C-scan from the front side, (b, d) C-scan from the backside, (a, b) unpinned laminate, (c, d) Z-pinned laminate.

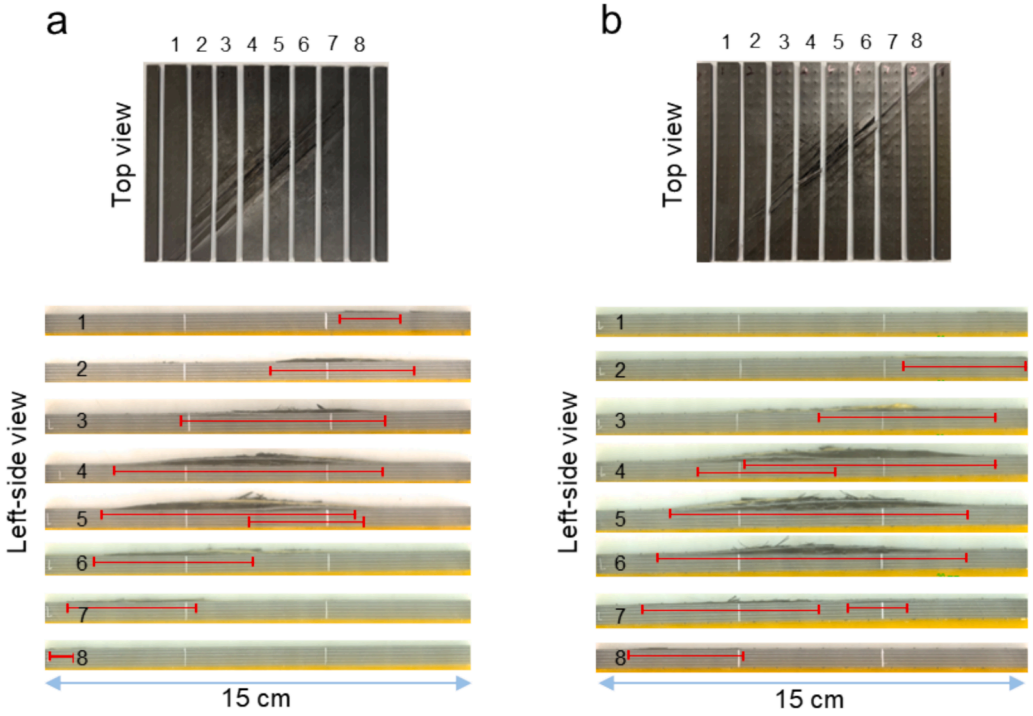

Fig. 4. The cross-section observation: (a) unpinned and (b) Z-pinned laminates. Note: The side-view images are stretched along the thickness direction for better visualisation.

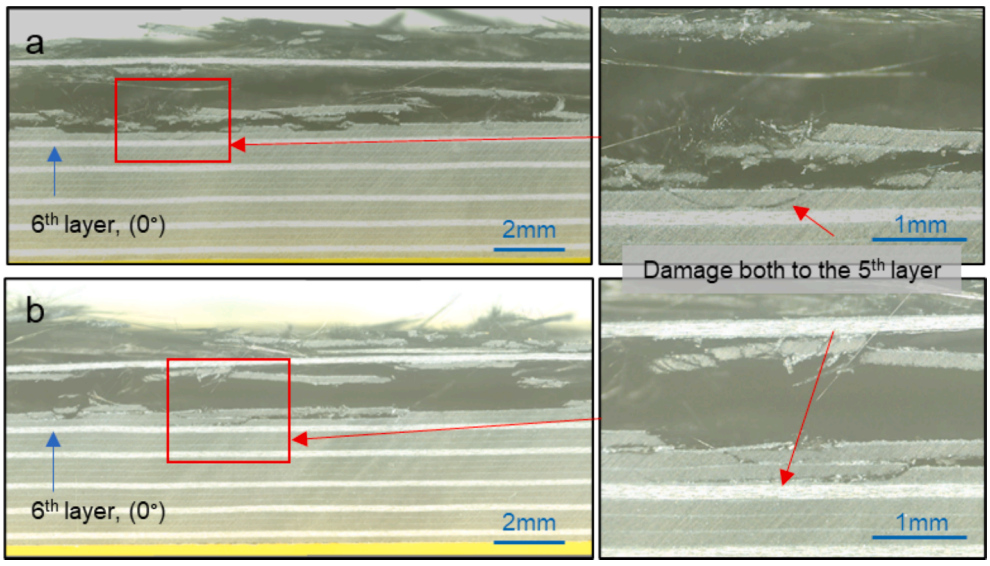

Fig. 5. The microscope image of the lightning strike centre area: (a) unpinned and (b) Z-pinned laminates.

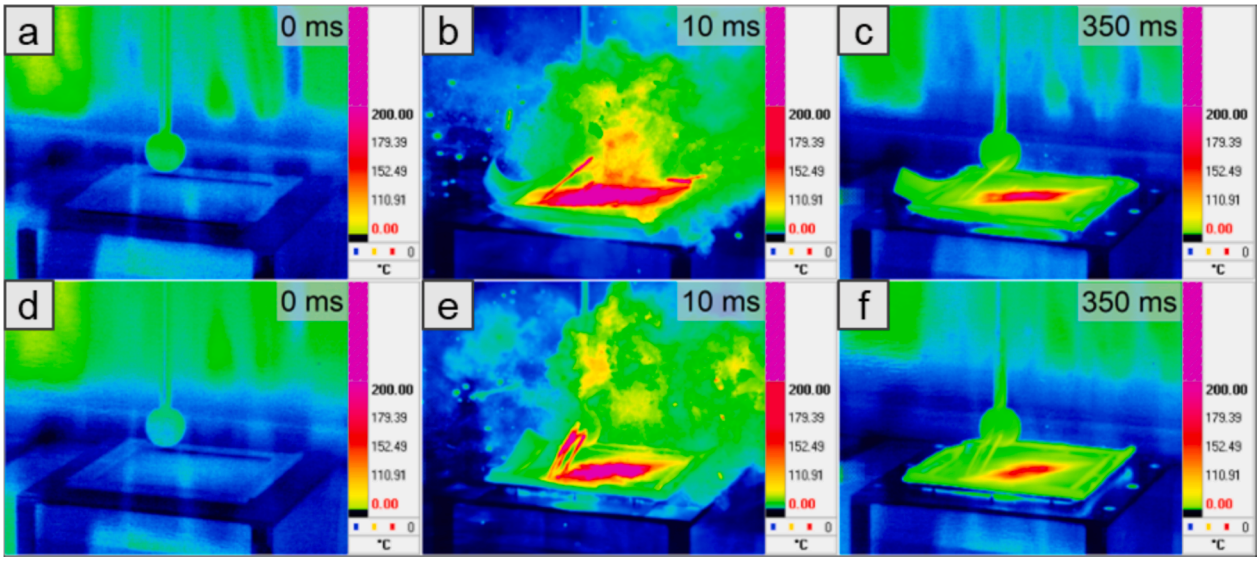

Fig. 6. The thermography images of unpinned (a–c) and Z-pinned (d–f) laminates during the lightning strike.

The generated pyrolysis gas was trapped in between layers and caused subsequently fibre peeling and delamination.

4.2. Non-destructive inspection

Ultrasonic C-scan was undertaken to gain a more comprehensive understanding of the damage inside the specimen. The scan utilised a pulse reflection technique, with a single probe systematically scanning the surface of the specimen along the X-Y axes. The ultrasonic defect detector used was the HIS3 HF model manufactured by Krautkramer GmbH, equipped with a 3.5 MHz transducer.

Fig. 3 displays the C-scan images. The pixel colours indicate the relative signal magnitude of the reflected waves. Blue pixels represent the baseline with a low amplitude reflected signal. Yellow and red pixels correspond to moderate and strong signal intensities, featuring mid-level and maximum amplitudes, respectively.

As depicted in Fig. 3(a, c), front-side scanning encounters significant attenuation due to damage in the surface layer, making it challenging to pinpoint the exact delaminated areas. The back-side C-scan images (Fig. 3(b, d)) exhibit distinct boundaries for the damaged region. It shows that the delamination in the second and third layers of the Z-pinned laminate is slightly larger compared to the unpinned one. This suggests that a greater amount of energy dissipated vertically into the deeper layers of the Z-pinned laminate, leading to more severe resin pyrolysis beneath the second and third layers. The resin pockets formed during the manufacturing of Z-pinned laminate is another major contributor to the larger delamination area, which will be discussed in Section 5.

4.3. Internal damage

To further investigate the actual damage length and depth, two specimens were repeated sliced at 16 mm intervals through the damaged zone, and their cross-section images were captured using a digital microscope, as depicted in Fig. 4. The visible delamination length is marked with red bars for clarity. Consistent with the C-scan results, larger delamination is observed in the first three layers of the Z-pinned laminate, as indicated by the length of the red bars. Closer images were

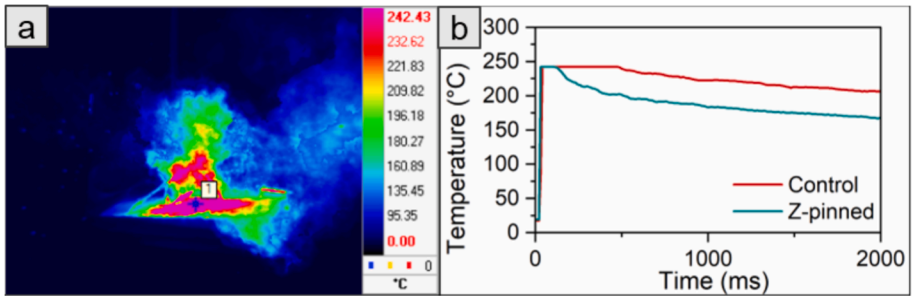

Fig. 7. (a) Illustration of the tracked centre point by thermal camera, and (b) temperature versus time plot of unpinned and Z-pinned laminates.

Table. 1
The through-thickness conductivity and lightning strike (LS) response in the present and previous studies.

Description	Conductivity	LS response	Ref.
Unpinned laminate	0.32 S/m	Fibre peeling and multiple layers delamination;	This study
Z-pinned laminate	10.8 S/m	Fibre peeling and multiple layers delamination;	This study
Conductive veils interleave	27.9 S/m	Two layers of damage;	[47]
Polyaniline conductive matrix	60 S/m	Minor surface ablation;	[21]
Silver-coated knitting yarns	627 S/m	Damage deeper than 1.0 mm reduced by 90%;	[13]
Copper tufting	5000 S/m	Comparable performance with copper mesh.	[20]

taken and carefully checked around the strike centre. As shown in Fig. 5, damage penetrated up to the fifth layer from the top in both control and Z-pinned laminates.

4.4. Thermography results

Thermography images captured by the thermal camera during the lightning strike test are displayed in Fig. 6. The time label in the upper right corner of each frame indicates the time since the lightning attachment. A threshold was applied to represent temperatures exceeding 200 °C as overheated areas (pink colour). A comparison of Fig. 6(b & e) and (c & f) reveals that the unpinned specimen exhibits larger hot zones than the Z-pinned one at the same timescale. This difference is attributed to the pins' effectiveness in dissipating heat flow in the through-thickness direction, as demonstrated in Refs. [15,33,35].

For a quantitative comparison, the temperature change at the laminate centre point (point 1 in Fig. 7(a)) is plotted in Fig. 7(b). The thermal camera operated at a frequency of 100 fps, capturing images every 10 ms, while the lightning strike test lasted for 0.09 ms. Thus, the curve illustrates the temperature change after the strike. It's worth noting that the highest temperature recorded during a lightning strike test exceeds 3000 °C [18,45,46], whereas the thermal camera's upper temperature limit was set at 250 °C. Therefore, the histogram presented here focuses exclusively on the cooling rate in the central region, i.e., the nonlinearly decreasing part of the curves.

Comparing the cooling rates of control and Z-pinned specimens, it is evident that the temperature of Z-pinned samples begins to decrease more rapidly than that of the control sample, thus maintaining the laminate in a safer condition after the lightning strike. This result again attributes to the enhanced heat dissipation, facilitated by the presence of the pins.

5. Damage mechanism discussion

5.1. Electrical conductivity

Electrical conductivity measurements were conducted prior to the lightning test in this study. The top and bottom surfaces of the specimens were carefully polished to remove the resin layer. The silver paste (DOTITE D-500, Fujikura Kasei Co., Ltd., Japan) was painted to the target surfaces and attach the aluminium electrodes. The specimens were thoroughly dried at 60 °C for one hour subsequently. An LCR metre (3522–50, Histester, Hioki EE Corporation, Ueda, Japan) was employed to measure the electrical resistance in the through-thickness direction.

As shown in Table. 1, the through-thickness electrical conductivity was enhanced by 33.8 times with Z-pins, which is consistent with the results in Ref. [29]. Numerous reports have emphasized the effectiveness of enhancing through-thickness electrical conductivity as a strategy to reduce lightning strike damage [13,20,21,47], as summarised in Table. 1. However, when dealing with Z-pinned laminates, it is essential to acknowledge that the conductivity testing method outlined in this paper, as well as in Ref. [29], may not precisely capture the through-thickness conductivity of the sample. This is because the sample's overall conductivity is predominantly attributed to the presence of the

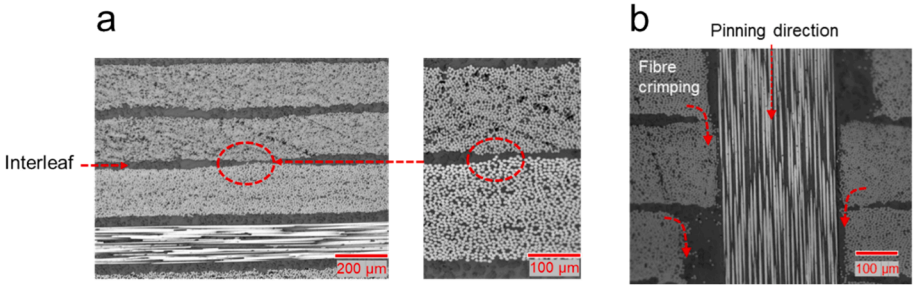

Fig. 8. Microscope images of sample cross-sections before lightning strike test: (a) unpinned, (b) carbon-fibre Z-pinned [15].

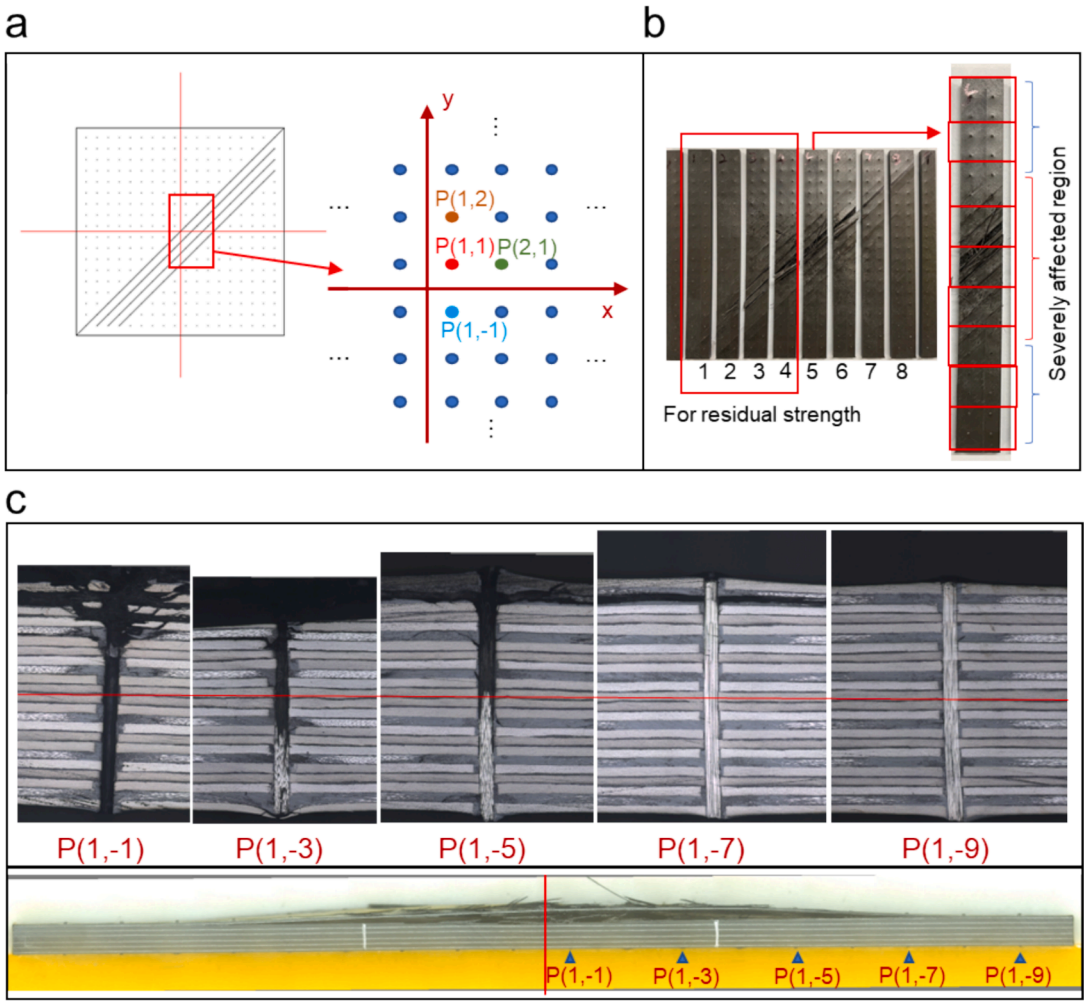

Fig. 9. (a) Numbering of the pins, (b) note of sample region classification, and (c) microscope images of the pin.

pins because electrodes covered the whole top and bottom surfaces. In practise, current may be injected through any location on the surface, and there exist cracks between the pins and host laminate, preventing direct current transfer from the laminate to the pins. This can explain why the lightning strike damage was not reduced, although the overall through-thickness conductivity was significantly improved by the pins. Therefore, a thorough analysis and understanding of the damage mechanism of those types of discrete reinforcement Z-pinning technology is of great importance.

5.2. Damage mechanism

The microscopic images of unpinned and Z-pinned specimens before the lightning strike test were reported in Ref. [15], as shown in Fig. 8. The current study uses the same specimen type, with identical material, manufacturing method, and pinning areal density. Fig. 8(a) presents an image of the unpinned specimen, where the interleaf with varying thicknesses is visible, along with randomly localised interlaminar fibre contacts within it. In contrast, for the Z-pinned specimen in Fig. 8(b), localised fibre crimping is observed, which could facilitate the transfer of a small and stable current in the through-thickness direction. However, the pin and laminate remain isolated due to interfacial cracks [15,29].

To investigate the damage mechanism of the Z-pinned laminate against lightning strike, the failure of individual pins inside the specimen was examined through microscopic observation. For better understanding, the pins were numbered according to their x and y coordinates as shown in Fig. 9(a), with the origin of the coordinate system at the lightning strike location.

Half of the No. 5 central strip was carefully cut and polished to reveal the pins in the most severely affected region, as depicted in Fig. 9(b). The microscope images in Fig. 9(c) illustrate that the central pin, P (1, −1), was completely burned off by the lightning strike, with the damage to the pins decreasing progressively from the centre to the edge, as observed in the images from P (1, −1) to P (1, −9). Fig. 10(a–c) provides detailed information about the partially burned pin P (1, −2). In Fig. 10 (a), the image displays both the tip and the transition region (from partially burned to intact) of the pin. Fig. 10(c) reveals the decomposition of a portion of the resin pocket region, highlighted within rectangular boxes. The resin pocket is a critical feature of Z-pinned laminates, as extensively discussed in the literature [4,5].

The other half of the No. 5 central strip was examined from the top using a scanning electron microscope (SEM). The SEM images in Fig. 10 (d–g) were captured in the vicinity of the pinning hole of P (1, 2). Fig. 10 (d, e) present top views of P (1, 2) after peeling off the first and third layers, respectively, while Fig. 10(f, g) are SEM images of polished top surfaces. These images distinctly reveal that the resin pockets surrounding the pin were either entirely or partially decomposed. This illustrates that electrical current indeed passed through the pins during the lightning strike event. Since the pin is composed of carbon fibre and BMI resin, the current flow through the pin, resulted in an immediate and intense Joule heating effect and followed by its breakdown into the resin pockets. This effect, in turn, led to the decomposition of both the BMI resin and the surrounding epoxy resin pockets.

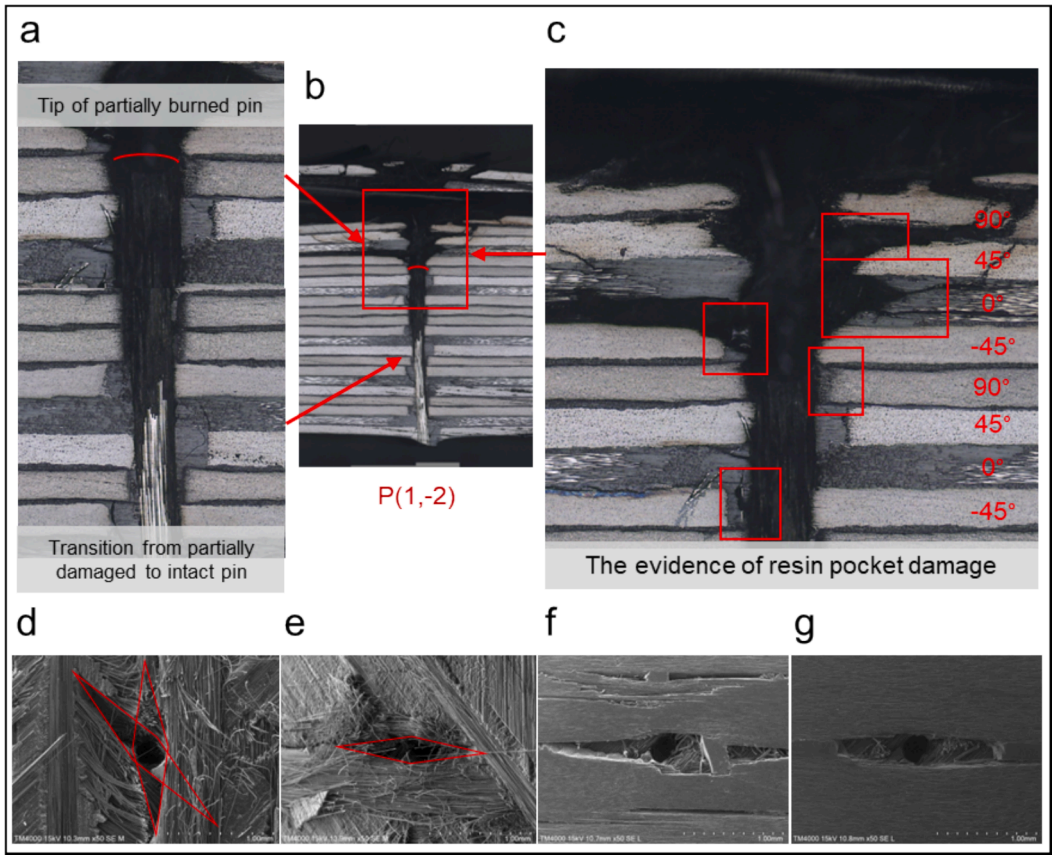

Fig. 10. (a-c) Microscope images of the surrounding regions of a partially burned off pin, (d-g) SEM images showing resin pockets' decomposition around the pins.

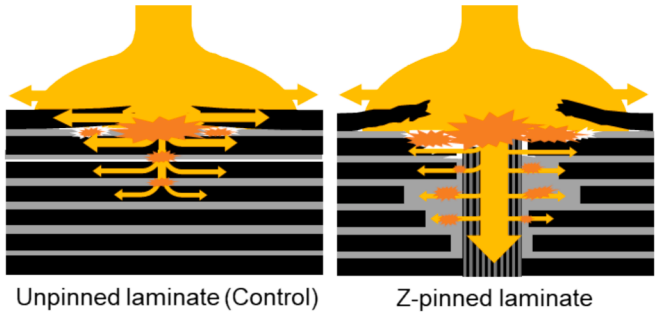

Fig. 11. Schematic illustration of the current path of the unpinned and Z-pinned laminates during the lightning strike.

A schematic illustration, shown in Fig. 11, reveals the current conducting pathways for both unpinned and Z-pinned specimens when exposed to a lightning strike. In the case of the unpinned laminate, current is solely conducted through the fibres. Due to the presence of interlaminar resin layers, the current only breaks down through several top plies. For the Z-pinned laminate, the current passed through the pins in the through-thickness direction. The instantaneous current surge during the lightning strike event is tremendous, and the heat surge of Joule heating causes the burning of pins and adjacent resin pockets. As a result, the high-pressure pyrolysis gas trapped inside each layer, or resin pocket, eventually caused more serious localised damage than the unpinned specimen.

6. Residual mechanical properties

Apart from the damage size and depth, the influence of the simulated

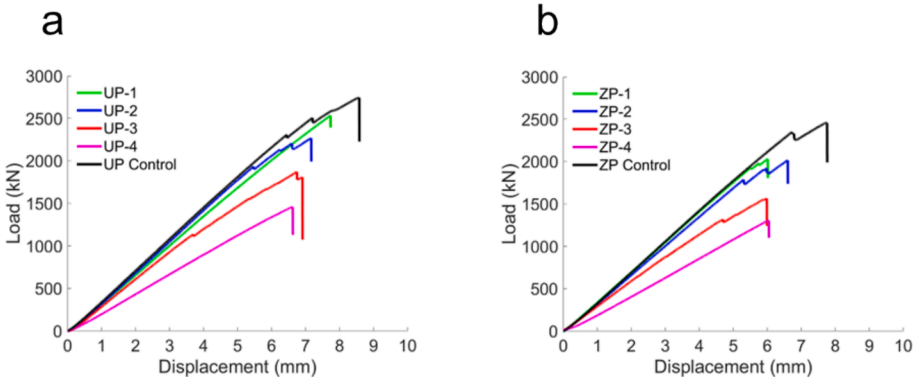

Fig. 12. Load-displacement curves of: (a) unpinned and (b) Z-pinned specimens for the four-point bending test.

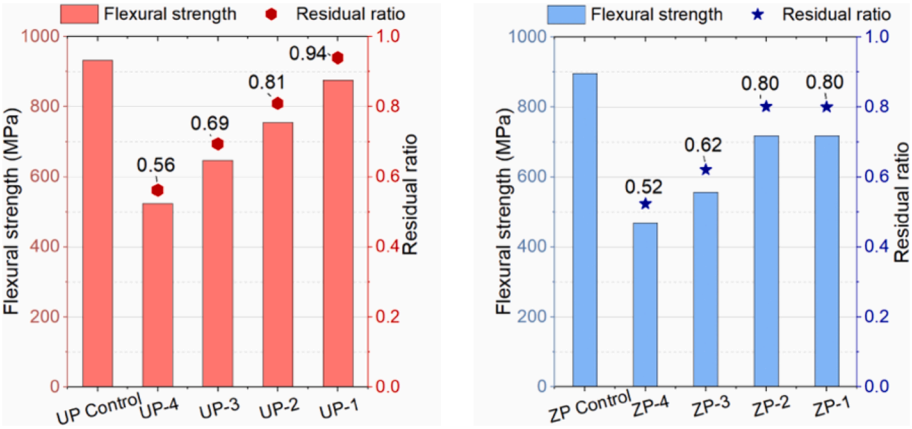

Fig. 13. The residual mechanical properties comparison between unpinned (UP) and Z-pinned (ZP) specimens.

lightning strikes is also evaluated by residual strength and stiffness, i.e., how much strength and stiffness the structure is able to retain compared to the reference sample without damage [12]. Four-point bending tests were carried out on 150 mm × 16 mm specimens cut from reference and tested panels (Fig. 9(b)), to assess their flexural strength. The lower span is 106 mm, while the upper span is one-third of this length. In the bending test, the lightning strike side is positioned on the compression side to enable a reasonable comparison of the residual mechanical properties. It was observed that all specimens failed due to compression failure.

The load–displacement curves are presented in Fig. 12. For specimens located further from the lightning strike centre (Nos. 1 and 2), there is a slight reduction in stiffness. However, for specimens closer to the strike centre, the reduction is more pronounced due to pre-existing damage caused by the lightning strike test. The residual stiffness of Z-pinned specimens is slightly lower than that of unpinned specimens.

The residual flexural strength, corresponding to the maximum load, is plotted in Fig. 13. It shows that the control laminate exhibits slightly higher pristine flexural strength than the Z-pinned specimen, which is due to the in-plane mechanical property reduction caused by the microstructural features induced by Z-pins [48,49]. The residual strength increases from the strike centre to the edge for both unpinned and Z-pinned laminates. The unpinned specimen closest to the strike centre (UP-4) exhibits a residual ratio of 56%, while the corresponding Z-pinned one (ZP-4) measures 52%. For the specimens (UP-3 and ZP-3) located the second closest to the strike centre, their residual ratios are 69% and 62%, respectively. Overall, the residual ratios of unpinned and Z-pinned laminates are close, further demonstrating that these two specimens showed a comparable extent of damage due to the high-current loading. The minor difference can be attributed to microstructural variations, as the decomposition of resin pockets and pins resulted in more localised damage to the laminate.

7. Conclusions

The effects of Z-pins on the lightning striking response of CFRP composites have been investigated experimentally. The visual damage is similar for the unpinned and Z-pinned specimens with fibre peeling along the fibre direction on the surface. Ultrasonic C-scan results show that Z-pinned laminate exhibits larger delamination area in the second and third layers compared to the unpinned one. The delamination penetrates to the fifth layer for both unpinned and Z-pinned laminates. This study demonstrated that while Z-pins enhanced overall through-thickness electrical conductivity, the decomposition of resin pockets and pins during electrical current surges generated trapped high-pressure pyrolysis gas, leading to severe localised damage. However, the Z-pinned laminate exhibited enhanced heat dissipation following the lightning strike, owing to the efficient heat transfer facilitated by the pins.

This work provides a new perspective on designing aircraft structural components, which require the use of the Z-pinning technique. In the future, it would be beneficial to consider increasing the pinning areal density or employing more conductive pins (e.g. copper), although such adjustments could potentially compromise the lightweight advantages inherent to CFRP.

CRediT authorship contribution statement

Mudan Chen: Writing – original draft, Validation, Methodology, Investigation, Funding acquisition, Formal analysis, Conceptualization. **Yu Zhou:** Writing – original draft, Validation, Methodology, Investigation, Formal analysis. **Bing Zhang:** Writing – review & editing, Supervision, Methodology, Conceptualization. **Giuliano Allegri:** Writing – review & editing, Supervision, Methodology, Conceptualization. **Tomohiro Yokozeki:** Writing – review & editing, Supervision, Project administration, Methodology. **Stephen R. Hallett:** Writing – review & editing, Supervision, Project administration, Methodology, Conceptualization.

Declaration of competing interest

The authors declare that they have no known competing financial interests or personal relationships that could have appeared to influence the work reported in this paper.

Acknowledgements

This work was funded by the Engineering and Physical Sciences Research Council (EPSRC) through the International Placement Scheme within the Centre for Doctoral Training in Advanced Composites for Innovation and Science [grant number EP/L016028/1], and the Japan Society for the Promotion of Science [JSPS Grant-in-Aid for Scientific Research, 21H01525].

The authors also would like to give credit to Mr. Takeo Sonehara from Shoden corporation, Dr. Takao Okada, Dr. Shintaro Kamiyama and Mr. Katsunori Takida from Japan Aerospace Exploration Agency (JAXA), and Mr. Xiaodong Li from the University of Tokyo for technical support for the simulated lightning strike test.

Data availability

Data will be made available on request.

References

[1] Dransfield K, Baillie C, Mai Y-W. Improving the delamination resistance of CFRP by stitching—a review. Compos Sci Technol 1994;50:305–17. https://doi.org/10.1016/0266-3538(94)90019-1.

[2] Dell'Anno G, Treiber JWG, Partridge IK. Manufacturing of composite parts reinforced through-thickness by tufting. Rob Comput Integr Manuf 2016;37:262–72. https://doi.org/10.1016/j.rcim.2015.04.004.

[3] Gerlach R, Siviour CR, Wiegand J, Petrinic N. In-plane and through-thickness properties, failure modes, damage and delamination in 3D woven carbon fibre composites subjected to impact loading. Compos Sci Technol 2012;72:397–411. https://doi.org/10.1016/j.compscitech.2011.11.032.

[4] Mouritz AP. Review of z-pinned laminates and sandwich composites. Compos A Appl Sci Manuf 2020;139:106128. https://doi.org/10.1016/j.compositesa.2020.106128.

[5] Mouritz AP. Review of z-pinned composite laminates. Compos A Appl Sci Manuf 2007;38:2383–97. https://doi.org/10.1016/j.compositesa.2007.08.016.

[6] Bianchi F, Zhang X. A cohesive zone model for predicting delamination suppression in z-pinned laminates. Compos Sci Technol 2011;71:1898–907. https://doi.org/10.1016/j.compscitech.2011.09.004.

[7] Yasaee M, Lander JK, Allegri G, Hallett SR. Experimental characterisation of mixed mode traction–displacement relationships for a single carbon composite Z-pin. Compos Sci Technol 2014;94:123–31. https://doi.org/10.1016/j.compscitech.2014.02.001.

[8] Pingkarawat K, Mouritz AP. Comparative study of metal and composite z-pins for delamination fracture and fatigue strengthening of composites. Eng Fract Mech 2016;154:180–90. https://doi.org/10.1016/j.engfracmech.2016.01.003.

[9] Cui H, Mahadik Y, Hallett SR, Partridge IK, Allegri G, Ponnusami SA, et al. Coupon scale Z-pinned IM7/8552 delamination tests under dynamic loading. Compos A Appl Sci Manuf 2019;125:105565. https://doi.org/10.1016/j.compositesa.2019.105565.

[10] Melro AR, Serra J, Allegri G, Hallett SR. An energy-equivalent bridging map formulation for modelling delamination in through-thickness reinforced composite laminates. Int J Solids Struct 2020;202:153–65. https://doi.org/10.1016/j.ijsolstr.2020.06.018.

[11] Santana de Vega E, Allegri G, Zhang B, Hamerton I, Hallett SR. Improving the delamination bridging performance of Z-pins through the use of a ductile matrix. Compos A Appl Sci Manuf 2022;163:107241. https://doi.org/10.1016/j.compositesa.2022.107241.

[12] Das S, Yokozeki T. A brief review of modified conductive carbon/glass fibre reinforced composites for structural applications: Lightning strike protection, electromagnetic shielding, and strain sensing. Composites, Part C: Open Access 2021;5:100162. https://doi.org/10.1016/j.jcomc.2021.100162.

[13] Rehbein J, Wierach P, Gries T, Wiedemann M. Improved electrical conductivity of NCF-reinforced CFRP for higher damage resistance to lightning strike. Compos A Appl Sci Manuf 2017;100:352–60. https://doi.org/10.1016/j.compositesa.2017.05.014.

[14] Yousefpour K, Lin W, Wang Y, Park C. Discharge and ground electrode design considerations for the lightning strike damage tolerance assessment of CFRP matrix composite laminates. Compos B Eng 2020;198:108226. https://doi.org/10.1016/j.compositesb.2020.108226.

[15] Chen M, Zhang Z, Zhang B, Allegri G, Yuan X, Hallett SR. Electrical and thermal behaviour of Z-pin reinforced carbon-fibre composite laminates under fault currents. Compos Sci Technol 2024;248:110466. https://doi.org/10.1016/j.compscitech.2024.110466.

[16] Piche A, Andissac D, Revel I, Lepetit B. Dynamic electrical behaviour of a composite material during a short circuit. In: 10th International Symposium on Electromagnetic Compatibility. IEEE; 2011. p. 128–32.

[17] Jones CE, Norman PJ, Sztykiel M, Pena Alzola R, Burt GM, Galloway SJ, et al. Electrical and thermal effects of fault currents in aircraft electrical power systems with composite aerostructures. IEEE Trans Transp Electrific 2018;4:660–70. https://doi.org/10.1109/TTE.2018.2833838.

[18] Ogasawara T, Hirano Y, Yoshimura A. Coupled thermal–electrical analysis for carbon fiber/epoxy composites exposed to simulated lightning current. Compos A Appl Sci Manuf 2010;41:973–81. https://doi.org/10.1016/j.compositesa.2010.04.001.

[19] Kamiyama S, Hirano Y, Ogasawara T. Delamination analysis of CFRP laminates exposed to lightning strike considering cooling process. Compos Struct 2018;196:55–62. https://doi.org/10.1016/j.compstruct.2018.05.003.

[20] Lombetti DM, Skordos AA. Lightning strike and delamination performance of metal tufted carbon composites. Compos Struct 2019;209:694–9. https://doi.org/10.1016/j.compstruct.2018.11.005.

[21] Zhou Y, Raghu SNV, Kumar V, Okada T, Yokozeki T. Simulated lightning strike investigation of CFRP comprising a novel polyaniline/phenol based electrically conductive resin matrix. Compos Sci Technol 2021;214:108971. https://doi.org/10.1016/j.compscitech.2021.108971.

[22] Hirano Y, Yokozeki T, Ishida Y, Goto T, Takahashi T, Qian D, et al. Lightning damage suppression in a carbon fiber-reinforced polymer with a polyaniline-based conductive thermoset matrix. Compos Sci Technol 2016;127:1–7. https://doi.org/10.1016/j.compscitech.2016.02.022.

[23] Kumar V, Yokozeki T, Okada T, Hirano Y, Goto T, Takahashi T, et al. Polyaniline-based all-polymeric adhesive layer: An effective lightning strike protection technology for high residual mechanical strength of CFRPs. Compos Sci Technol 2019;172:49–57. https://doi.org/10.1016/j.compscitech.2019.01.006.

[24] Rajesh PSM, Sirois F, Therriault D. Damage response of composites coated with conducting materials subjected to emulated lightning strikes. Mater Des 2018;139:45–55. https://doi.org/10.1016/j.matdes.2017.10.017.

[25] Kumar V, Sharma S, Pathak A, Singh BP, Dhakate SR, Yokozeki T, et al. Interleaved MWCNT buckypaper between CFRP laminates to improve through-thickness electrical conductivity and reducing lightning strike damage. Compos Struct 2019;210:581–9. https://doi.org/10.1016/j.compstruct.2018.11.088.

[26] Xia Q, Zhang Z, Liu Y, Leng J. Buckypaper and its composites for aeronautic applications. Compos B Eng 2020;199:108231. https://doi.org/10.1016/j.compositesb.2020.108231.

[27] Zhang B, Allegri G, Yasaee M, Hallett SRR, Partridge IKK. On the delamination self-sensing function of Z-pinned composite laminates. Compos Sci Technol 2016;128:138–46. https://doi.org/10.1016/j.compscitech.2016.03.019.

[28] Zhang B, Allegri G, Hallett SR. An experimental investigation into multi-functional Z-pinned composite laminates. Mater Des 2016;108:679–88. https://doi.org/10.1016/j.matdes.2016.07.035.

[29] Pegorin F, Pingkarawat K, Mouritz AP. Controlling the electrical conductivity of fibre-polymer composites using z-pins. Compos Sci Technol 2017;150:167–73. https://doi.org/10.1016/j.compscitech.2017.07.018.

[30] Pegorin F, Pingkarawat K, Mouritz AP. Electrical-based delamination crack monitoring in composites using z-pins. Compos A Appl Sci Manuf 2018;104:120–8. https://doi.org/10.1016/j.compositesa.2017.10.025.

[31] Pegorin F, Pingkarawat K, Mouritz AP. Numerical analysis of the heat transfer properties of z-pinned composites. Compos Commun 2018;8:14–8. https://doi.org/10.1016/j.coco.2018.03.002.

[32] Grigoriou K, Ladani RB, Mouritz AP. Electrical properties of multifunctional Z-pinned sandwich composites. Compos Sci Technol 2019;170:60–9. https://doi.org/10.1016/j.compscitech.2018.11.030.

[33] Li M, Fang Z, Wang S, Gu Y, Li Y, Zhang Z. Thermal conductivity enhancement and heat transport mechanism of carbon fiber z-pin graphite composite structures. Compos B Eng 2019;172:603–11. https://doi.org/10.1016/J.COMPOSITESB.2019.05.092.

[34] Kadlec M, Růžek R, Bělský P. Concurrent use of Z-pins for crack arrest and structural health monitoring in adhesive-bonded composite lap joints. Compos Sci Technol 2020;188:107967. https://doi.org/10.1016/J.COMPSCITECH.2019.107967.

[35] Li M, Fang Z, Wang S, Gu Y, Zhang W. Thermal conductivity enhancement and synergistic heat transfer of z-pin reinforced graphite sheet and carbon fiber hybrid composite. Int J Heat Mass Transf 2021;171:121093. https://doi.org/10.1016/j.ijheatmasstransfer.2021.121093.

[36] Zhang B, Hallett SR, Allegri G. Sensing delamination in composites reinforced by ferromagnetic Z-pins via electromagnetic induction. Compos Sci Technol 2022;217:109113. https://doi.org/10.1016/j.compscitech.2021.109113.

[37] Chen M, Zhang B, Friedemann S, Allegri G, Hallett SR. Effects of ferromagnetic & carbon-fibre Z-Pins on the magnetic properties of composites. Compos Sci Technol 2021;207:108749. https://doi.org/10.1016/j.compscitech.2021.108749.

[38] HexPly_M21_global_DataSheet.pdf; 2022. https://www.hexcel.com.

[39] Sfar Zbed R, Le Corre S, Sobotka V. Process-induced strains measurements through a multi-axial characterization during the entire curing cycle of an interlayer toughened Carbon/Epoxy prepreg. Compos A Appl Sci Manuf 2022;153:106689. https://doi.org/10.1016/j.compositesa.2021.106689.

[40] Bilge K, Papila M. Interlayer toughening mechanisms of composite materials. Toughening Mechanisms in Composite Materials 2015:263–94. https://doi.org/10.1016/B978-1-78242-279-2.00010-X.

[41] Chen M, Zhang B, Allegri G, Hallett SR. Effects of carbon-fibre Z-pins on the through-thickness tensile strength of curved composite laminates under four-point bending. Compos B Eng 2024;283:111629. https://doi.org/10.1016/j.compositesb.2024.111629.

[42] Chemartin L, Lalande P, Peyrou B, Chazottes A, Elias PQ, Delalondre C, et al. Direct effects of lightning on aircraft structure: analysis of the thermal, electrical and mechanical constraints. Aerosp Lab 2012:1–15.

[43] Wang FS, Ding N, Liu ZQ, Ji YY, Yue ZF. Ablation damage characteristic and residual strength prediction of carbon fiber/epoxy composite suffered from lightning strike. Compos Struct 2014;117:222–33. https://doi.org/10.1016/j.compstruct.2014.06.029.

[44] Wang B, Zhu Y, Ming Y, Yao X, Tian X, Ziegmann G, et al. Understanding lightning strike induced damage mechanism of carbon fiber reinforced polymer composites: an experimental study. Mater Des 2020;192:108724. https://doi.org/10.1016/j.matdes.2020.108724.

[45] Abdelal G, Murphy A. Nonlinear numerical modelling of lightning strike effect on composite panels with temperature dependent material properties. Compos Struct 2014;109:268–78. https://doi.org/10.1016/j.compstruct.2013.11.007.

[46] NASA - NASA Lightning Research Highlights Safety Awareness Week n.d. https://www.nasa.gov/vision/earth/lookingatearth/lightning_wk_2006.html.

[47] Zhao ZJ, Xian GJ, Yu JG, Wang J, Tong JF, Wei JH, et al. Development of electrically conductive structural BMI based CFRPs for lightning strike protection. Compos Sci Technol 2018;167:555–62. https://doi.org/10.1016/j.compscitech.2018.08.026.

[48] Chang P, Mouritz AP, Cox BN. Flexural properties of z-pinned laminates. Compos A Appl Sci Manuf 2007;38:244–51. https://doi.org/10.1016/j.compositesa.2006.05.004.

[49] Mouritz AP, Cox BN. A mechanistic interpretation of the comparative in-plane mechanical properties of 3D woven, stitched and pinned composites. Compos A Appl Sci Manuf 2010;41:709–28. https://doi.org/10.1016/j.compositesa.2010.02.001.